



This is a repository copy of *Major histocompatibility complex class I molecules protect motor neurons from astrocyte-induced toxicity in amyotrophic lateral sclerosis*.

White Rose Research Online URL for this paper:
<http://eprints.whiterose.ac.uk/105459/>

Version: Accepted Version

Article:

Song, S., Miranda, C. J., Braun, L. et al. (9 more authors) (2016) Major histocompatibility complex class I molecules protect motor neurons from astrocyte-induced toxicity in amyotrophic lateral sclerosis. *Nature Medicine*, 22. pp. 397-403. ISSN 1078-8956

<https://doi.org/10.1038/nm.4052>

Reuse

Unless indicated otherwise, fulltext items are protected by copyright with all rights reserved. The copyright exception in section 29 of the Copyright, Designs and Patents Act 1988 allows the making of a single copy solely for the purpose of non-commercial research or private study within the limits of fair dealing. The publisher or other rights-holder may allow further reproduction and re-use of this version - refer to the White Rose Research Online record for this item. Where records identify the publisher as the copyright holder, users can verify any specific terms of use on the publisher's website.

Takedown

If you consider content in White Rose Research Online to be in breach of UK law, please notify us by emailing eprints@whiterose.ac.uk including the URL of the record and the reason for the withdrawal request.



eprints@whiterose.ac.uk
<https://eprints.whiterose.ac.uk/>



HHS Public Access

Author manuscript

Nat Med. Author manuscript; available in PMC 2016 August 29.

Published in final edited form as:

Nat Med. 2016 April ; 22(4): 397–403. doi:10.1038/nm.4052.

MHC class I protects motor neurons from astrocyte-induced toxicity in amyotrophic lateral sclerosis (ALS)

SungWon Song^{#1,2}, Carlos J. Miranda^{#1}, Lyndsey Braun¹, Kathrin Meyer¹, Ashley E. Frakes^{1,3}, Laura Ferraiuolo¹, Shibi Likhite^{1,2}, Adam K. Bevan^{1,3}, Kevin D. Foust^{1,4}, Michael J. McConnell⁵, Christopher M. Walker^{6,7}, and Brian K. Kaspar^{1,2,3,4,7}

¹ Center for Gene Therapy, The Research Institute at Nationwide Children's Hospital, Columbus, Ohio, USA

² Molecular, Cellular & Developmental Biology Graduate Program, The Ohio State University, Columbus, Ohio, USA

³ Biomedical Sciences Graduate Program, The Ohio State University, Columbus, Ohio, USA

⁴ Department of Neuroscience, The Ohio State University, Columbus, Ohio, USA

⁵ Dept. of Biochemistry and Molecular Genetics, University of Virginia, Charlottesville, Virginia, USA

⁶ Center for Vaccines and Immunity, The Research Institute at Nationwide Children's Hospital, Columbus, Ohio, USA

⁷ Department of Pediatrics, College of Medicine and Public Health, The Ohio State University, Columbus, Ohio, USA

These authors contributed equally to this work.

Abstract

Astrocytes isolated from individuals with amyotrophic lateral sclerosis (ALS) are toxic towards motor neurons (MNs) and play a non-cell autonomous role in disease pathogenesis. The mechanisms underlying the susceptibility of motor neurons to cell death remains unclear. Here, we report that astrocytes derived from mice bearing ALS mutations and from individuals with ALS

Users may view, print, copy, and download text and data-mine the content in such documents, for the purposes of academic research, subject always to the full Conditions of use:http://www.nature.com/authors/editorial_policies/license.html#terms

To whom correspondence should be addressed. Brian K. Kaspar, Ph.D., ; Email: Brian.Kaspar@NationwideChildrens.org

Author contributions All authors contributed to the design of the experiments. Mouse astrocyte, microglia and NPC isolation was performed by S. Song, C. J. Miranda, L. Braun, A. Frakes and S. Likhite. Human astrocytes cultures were performed by S. Song, C. J. Miranda, K. Meyer, and L. Ferraiuolo. Neuronal cell differentiation and co-culture experiments were performed by S. Song, C. J. Miranda, K. Meyer, A. Frakes and S. Likhite. *In situ* hybridization of H2d^b transcripts was performed by M. J. McConnell. RT-PCR and immunocytochemistry were performed by S. Song, C. J. Miranda, L. Braun, and A. K. Bevan. Lentivirus production was performed by S. Song, C. J. Miranda, L. Braun, K. Meyer, A. Frakes, L. Ferraiuolo, and S. Likhite. Data analysis was performed by S. Song, C. J. Miranda, L. Braun, K. Meyer, A. Frakes, L. Ferraiuolo, S. Likhite, A. K. Bevan, K. D. Foust, M. J. McConnell, C. M. Walker, and B. K. Kaspar. The manuscript and figures were prepared by S. Song, C. J. Miranda, and B. K. Kaspar with input from all co-authors.

Supplementary Information is available in the online version of the paper.

Competing financial interests

The authors declare no competing financial interests.

reduce expression of major histocompatibility complex class I (MHCI) on MNs. Reduced MHCI expression makes these MNs susceptible to astrocyte-induced cell death. Increasing MHCI expression on MNs increases survival and motor performance in a mouse model of ALS and protects MN against astrocyte toxicity. A single MHCI molecule, *HLA-F*, protects MNs from ALS astrocyte-mediated toxicity, while knockdown of its receptor, the killer cell immunoglobulin-like receptor *KIR3DL2*, an inhibitory receptor that recognizes MHCI, on astrocytes results in enhanced MN death. These data indicate that in ALS upon loss of MHCI expression MNs become vulnerable to astrocyte-mediated toxicity.

Introduction

Amyotrophic lateral sclerosis (ALS) is a fatal, adult onset neurodegenerative disorder characterized by the progressive loss of motor neurons (MNs) and death due to respiratory failure¹. The majority of cases are classified as sporadic ALS (SALS), defined as having no family history of the disease. Despite efforts to identify risk factors and potential susceptibility genes, the etiology of SALS remains largely unknown². Current understanding of cellular and molecular mechanisms underlying this disease is mostly derived from animals models bearing mutations in genes associated with autosomal dominant familial ALS (FALS)³⁻⁷. Despite the difference in etiology, FALS and SALS are phenotypically indistinguishable. Several studies suggest a common disease mechanism underlying FALS and SALS^{8,9} and therefore knowledge gathered from animal models of FALS can help understand the mechanism behind SALS¹⁰.

In addition to cell intrinsic damage occurring within MNs, glial cells such as astrocytes, microglia and oligodendrocytes contribute to MN death in ALS in a non-cell autonomous manner^{11,12}. Astrocytes derived from postmortem biopsies of human ALS individuals induce MN death *in vitro*, opening the possibility to study these patient specific cells in great detail^{13,14}. However, the understanding of how and why MNs die in this disease remains unknown.

Recent work in development, aging and neurological disorders, including ALS has focused on immune molecules, such as cytokines, proteins of the complement system, and major histocompatibility complex class I (MHCI) proteins and their role in the developing and adult brain^{15,17}. In the central nervous system (CNS), MHCI plays a role in synaptic function^{15,18,22}, and in neurodegenerative processes^{23,24}. In the ALS mouse model, which express a disease-associated variant in superoxide dismutase 1 (*SOD1*^{G93A}) mice, higher levels of MHCI in MNs were found in animals that presented a slower disease progression²⁵. Furthermore, disease progression is accelerated in *SOD1*^{G93A} mice lacking beta-2 microglobulin (β 2m), an essential component for MHCI presentation²⁶. Taken together these findings suggest that MHCI may have a role in the pathogenesis of ALS.

Results

MHCI expression is reduced on MNs in ALS

MHCI molecules and $\beta 2m$ are enriched in mouse spinal MNs (**Supplementary Fig. 1a,b**). In order to examine changes in MHCI expression in MNs in ALS, we analyzed MHCI expression prior to and after disease onset in all segments of the spinal cord of *SOD1*^{G93A} mice and compared them to wild-type mice. Using an antibody that recognizes subgroups of mouse MHCI (histocompatibility 2 (H2), *k^b* and *d^b*) and commonly used for MHCI detection in MNs^{25,27}, we found that MHCI expression was markedly reduced in MN somata but increased in motor axons in *SOD1*^{G93A} mice after disease onset (**Fig. 1a,b** and **Supplementary Fig. 1c-e**). These results are in agreement with previous findings using another rapid progressing *SOD1* mouse model (129Sv-*SOD1*^{G93A}) showing that MHCI protein is transported away from MN cell body and accumulates in peripheral motor axons during disease progression²⁵.

Next, to determine if loss of MHCI in MNs seen in the mouse model was also seen in human ALS individuals, we evaluated MHCI expression by immunohistochemistry in spinal cord samples from FALS carrying the *SOD1*^{A4V} mutation and sporadic ALS individuals compared to non-ALS controls. Using an antibody recognizing human leukocyte antigen (HLA)-A, -B, and -C, we observed that MHCI expression in MNs was nearly absent in both FALS and SALS spinal cords as compared to MHCI levels expression in MNs of non-ALS samples (**Fig. 1c,d**).

Loss of MHCI by MNs after exposure to ALS astrocytes

Using our recently described co-culture system of adult CNS derived microglia with MNs²⁸, we evaluated the impact of ALS microglia on the expression of MHCI in MNs. Although *SOD1*^{G93A} microglia have been shown to be toxic to MNs²⁸, when MNs were co-cultured with *SOD1*^{G93A} microglia, no overt changes were observed in their MHCI expression (**Fig. 2a**). By contrast when MNs were co-cultured with ALS astrocytes²⁹, confirmed to be devoid of other glia types or cytotoxic T lymphocytes (CTLs) and natural killer (NK) cells (**Supplementary Fig. 2a-g**), MHCI expression in MNs was diminished already within 24 hours and steadily declined over the next 96 hours, at which point approximately 73% of MNs completely lost MHCI expression (**Fig. 2b**). MHCI expression in MNs was slightly increased during the same period when MNs were cultured on top of wild-type astrocytes (**Fig. 2b**). This could reflect MN maturation in the presence of astrocytes³⁰, which affects MHCI expression patterns in neurons³¹.

In order to evaluate if expression of ALS linked-mutant *SOD1* protein within MNs could lead to intrinsic down-regulation of MHCI expression, we generated wild-type and *SOD1*^{G93A} MNs using induced pluripotent stem cell (iPSC) technology³². The iPSCs generated contained the green fluorescent protein (GFP) under the control of the MN specific Hb9 promoter allowing MN enrichment using a fluorescence activated cell sorter upon MN induced cell differentiation (**Supplementary Fig. 3a-b**)³². Upon confirming that both wild-type and *SOD1*^{G93A} iPSC showed neuronal morphology and gene expression profiles similar to MNs derived from mouse embryonic stem cells (**Supplementary Fig. 3c**),

MHCI levels were evaluated. During the first 72 hours, no significant change in MHCII expression was found between wild-type and *SOD1^{G93A}* MNs and only a modest down-regulation of MHCII was observed in *SOD1^{G93A}* MNs by 120 hour (**Supplementary Fig. 4a**). A further decrease was not observed if *SOD1^{G93A}* expressing MNs were culture in the presence of *SOD1^{G93A}* astrocytes (**Supplementary Fig. 4b**), suggesting that ALS astrocytes act as a main contributor to the down-regulation of MHCII observed in MNs. Of note, the findings described above were not observed in GABAergic neurons, a neuronal population spared from ALS astrocyte induced toxicity when co-cultured^{13,14,33,34}, since MHCII expression levels in these cells were found to remained constant throughout the culture period in the presence of *SOD1^{G93A}* astrocytes (**Supplementary Fig. 4c**).

Next, in order to determine if cell-cell contact between MNs and astrocytes was required for MHCII loss in MNs to occur, we cultured MNs in medium previously used to culture astrocytes but without physical contact with astrocytes. As observed in the presence *SOD1^{G93A}* astrocytes by 24 hours majority of MNs lost MHCII expression after culture with *SOD1^{G93A}* astrocyte conditioned medium a time point where at least 95% of MNs are still alive (**Supplementary Fig. 5a**), suggesting ALS astrocytes secrete factors that induce MHCII down-regulation in MNs. Based on these findings we then evaluated if we could recapitulate this down-regulation of MHCII in MNs observed in the presence of *SOD1^{G93A}* astrocyte conditioned medium by using compounds acting on pathways shown to be affected in ALS. Compounds causing endoplasmic reticulum (ER) stress, oxidative stress, and inflammatory response were tested. Thapsigargin, a sarco-endoplasmic reticulum calcium ATPase inhibitor, known to induce ER stress in MNs³⁵, led to loss of MHCII expression in more than 76% of MNs, where menadione, an oxidative stress inducer, and the pro-inflammatory molecules, tumor necrosis factor (TNF α), interferon gamma (IFN γ) and interleukin 2 (IL2) showed no or only moderate effects on MNs MHCII levels (**Supplementary Fig. 5b**). Taken together, these results suggest that astrocytes may secrete inducers of ER stress resulting in loss of MHCII in MNs.

Levels of MHCII in MN determine susceptibility to ALS astrocyte-induced toxicity

To test the hypothesis that restoring MHCII expression to MNs may prevent astrocyte mediated toxicity, we overexpressed three MHCII molecules in MNs prior to co-culture with mouse ALS astrocytes. Mouse classical MHCII of the subclasses *H2d^b*, *H2k^b* or *H2I^d* were overexpressed via lentiviral vectors in Hb9:GFP sorted MNs, resulting in transduction of more than 80% of MNs and rescue of MHCII levels on MNs exposed to *SOD1^{G93A}* astrocyte (**Supplementary Fig. 6a-d**)³⁶. While overexpression of *H2d^b* or *H2I^d* in MNs resulted in a modest increase in MN survival, overexpression of *H2k^b* fully protected MN from the toxic effects of *SOD1^{G93A}* astrocytes with no changes in cell morphology (**Fig. 3a**). This effect was not due to the lentivirus infection *per se* since expression of RFP did not alter *SOD1^{G93A}* astrocyte-mediated toxicity, with more than 60% of MNs dying within 120 hours of co-culture (**Fig. 3b**).

Knockdown of *H2k^b* expression in MN did not induce MN cell death *per se* or alter their susceptibility to stress molecules (**Supplementary Fig. 7a**), but upon co-culture with *SOD1^{G93A}* astrocytes increased susceptibility to *SOD1^{G93A}* astrocyte-induced toxicity

(**Supplementary Fig. 7b**). Importantly, reduction of MHC I expression in GABAergic neurons lead to decreased survival upon co-culture with *SOD1*^{G93A} astrocytes, with an observed 43.7% cell death as compared to scrambled shRNA transduced GABAergic neurons (**Supplementary Fig. 7c-e**). These findings suggest that MHCI expression by neuronal cells modulates their susceptibility to ALS astrocyte-induced toxicity.

Sustained *H2k* expression delayed *SOD1* disease progression

Since AAV9 readily transduces MNs in the spinal cord when delivered in to the cerebral spinal fluid (CSF)^{37,38}, we constructed AAV9 vectors to target MNs in *SOD1*^{G93A} mice with *H2k^b* (AAV9-*H2k*) or *H2d^b* (AAV9-*H2d*). We also used AAV9-*GFP* to confirm that high level of transduction in spinal cord MNs of *SOD1*^{G93A} mice could be achieved by our delivery method (**Supplementary Fig. 8a**). AAV9-*H2k* (or AAV9-*H2k*) increased *H2k^b* (or *H2d^b*) mRNA expression levels in spinal cords (**Supplementary Fig. 8b**). Expression of *H2k^b* in MNs via AAV9 delivery starting at post-natal day 1 resulted in a 21-day extension in the mean survival *SOD1*^{G93A} mice as compared to control (AAV9-empty) littermates (156.9 ± 2.6 days in AAV9-*H2k* versus 135.5 ± 1.6 days in AAV9-empty (**Fig. 3c**). Amongst AAV9-*H2k* injected animals, 39% of the animals survived over 165 days, with the longest living mouse reaching 182 days. When AAV9-*H2k* was delivered to *SOD1*^{G93A} mice, no significant ($P > 0.05$) changes in mean survival were observed (139.2 ± 1.4 days in AAV9-*H2k* versus 135.5 ± 1.6 days in AAV9-empty). Mean disease onset, as assessed by age at peak body weight did not differ between AAV9-*H2k*, AAV9-*H2k* and AAV9-empty groups (103.3 ± 2.0, 103.1 ± 1.2 and 99.73 ± 1.2 days, respectively; **Fig. 3d-e**). However, disease duration, assessed by disease progression, was increased by 50.3% in AAV9-*H2k* treated mice, but not in AAV9-*H2k* treated mice (**Fig. 3f**). Videos taken of *SOD1*^{G93A} mice during the disease progression period, show a marked difference between AAV9-*H2k* injected versus AAV9-empty injected mice (**Supplementary Videos 1-4**). During this stage, AAV9-*H2k* injected *SOD1*^{G93A} mice showed greater ambulatory capacity compared to AAV9-empty injected animals. Motor function was also improved as assessed by rotarod test (**Fig. 3g**). The delay in disease progression observed when *SOD1*^{G93A} mice were treated with AAV9-*H2k* is likely not derived from *H2k^b* expression in astrocytes since the overexpression of *H2k^b* in *SOD1*^{G93A} astrocytes *in vitro* did not modify their toxicity towards MNs (**Supplementary Fig. 9**).

ALS astrocytes express MHCI inhibitory receptors

The levels of MHCI expression helps innate immune cells, including natural killer (NK) cells, to distinguish target cells from healthy cells³⁹. Reduced presentation of MHCI antigen on target cells acts as a trigger for cytotoxic T lymphocytes (CTLs) to secrete effector molecules and kill the target cells⁴⁰. However, when target cells retain MHCI expression, CTLs can sense this MHCI leading to the engagement of signaling cascades that inhibit lymphocytic toxicity and result in the preservation of target cells^{40,41}. To determine if ALS astrocytes have the ability to sense MHCI levels on MNs, we examined expression of MHCI receptors in astrocytes. mRNA expression of H2k inhibitory receptors of the *Ly49* family such *Ly49c*, *Ly49i* and *Ly49w* were highly expressed *SOD1*^{G93A} mice at end stages of disease (**Fig. 4a**). Immunostaining analysis using antibodies to detect *Ly49c* and *Ly49i*

(Ly49c/i) receptors confirmed expression of these two receptors in the ventral horn of the lumbar spinal cord of *SOD1*^{G93A} mice, with little to no expression in age-matched wild-type mice (**Fig. 4b-c**). $96 \pm 2\%$ of Ly49c/i positive cells were astrocytes (defined by immunoreactivity to the astrocyte specific membrane protein GLAST or the cytoplasmic protein GFAP) (**Fig. 4c** and **Supplementary Fig. 10a**). Ly49c/i receptors were also expressed in *SOD1*^{G93A} astrocytes used in our *in vitro* studies (**Fig. 4d-e**). These receptors were also detected in infiltrating CTLs found in the spinal cord of *SOD1*^{G93A} mice⁴², however CTL numbers were minimal and therefore only accounted for a small fraction of cells expressing Ly49c/i receptors (**Supplementary Fig. 10b**).

We extended our analysis to astrocytes derived from individuals with ALS and analyzed mRNA expression of a wide panel of 14 MHC I receptors. Killer cell immunoglobulin-like receptor 3DL2 (*KIR3DL2*), an inhibitory MHC I receptor, was uniquely expressed in all human ALS astrocyte cell lines tested (**Fig. 4f**). There was no detectable expression of MHC I inhibitory receptor, including *KIR3DL2* or any other KIR in non-ALS control astrocyte cell lines tested. Expression of *KIR3DL2* was also confirmed in post-mortem spinal cord samples of SALS individuals, where *KIR3DL2* expression was predominantly localized to GFAP positive astrocytes (**Fig. 4g-h**).

***HLA-F* protects human MNs from ALS astrocyte toxicity**

Major histocompatibility complex, class I, F (*HLA-F*), a human MHC I molecule, has been identified as a ligand that can physically and functionally interact with the *KIR3DL2* receptor⁴³. *HLA-F* is expressed in MNs of non-ALS spinal cord samples, and its expression is reduced in ALS MNs (**Fig. 5a-b**). To test whether sustained expression of *HLA-F* in human MNs protects them from ALS astrocyte induced toxicity, we used an *in vitro* model system where human MNs and human astrocytes were co-cultured¹⁴. MNs were generated from human embryonic stem cells and found to exhibit good neuronal morphology, expression of the MN markers homeobox gene (HB9), neurofilament marker (SMI32) and choline acetyltransferase (ChAT) and minimal to none non-neuronal cell contamination (**Fig. 5c**). Given that MHC I recognition is species specific, we needed to construct a vector that could deliver *HLA-F* to human MNs. A lentiviral vector encoding human *HLA-F* cDNA along with an IRES and eGFP (*Lv-HLAF-IRES-eGFP*) to track transduced cells was produced. Transgene expression and high levels of MN transduction were confirmed, with a transduction efficiency of over 90% (**Fig. 5d**), and all cells expressing *eGFP* were found to express *HLA-F* (**Supplementary Fig. 11**). Three-days after the MNs were transduced with *Lv-HLAF-IRES-eGFP*, astrocytes devoid of contamination by other glia and CTLs, (**Supplementary Fig. 2d,e**) were added to cultures. After 2 weeks of co-culture we observed that overexpression of *HLA-F* in human derived MNs increased their survival upon co-culture with either FALS or SALS astrocytes (**Fig. 5e-f**). No change in MN survival was observed when MNs overexpressing *HLA-F* were co-cultured with non-ALS astrocytes, suggesting a specific effect of *HLA-F* in preventing ALS astrocyte mediated toxicity rather than improved general MN survival. To test whether suppression of *KIR3DL2* in ALS astrocytes will enhance their toxicity towards MNs, we reduced *KIR3DL2* expression in human astrocytes using shRNA directed against *KIR3DL2* (**Supplementary Fig. 12a**). All ALS astrocytes treated with scrambled shRNA were toxic to MNs, with approximate 50%

MNs death observed by day 14 (**Supplementary Fig. 12b**). When the same MNs were co-cultured with ALS astrocytes lacking *KIR3DL2* expression, 50% MN death could already be observed by day 7 of co-culture (**Supplementary Fig.12b**) suggesting an increase cell death activity of ALS astrocytes if they lack the functional interacting domain to *HLA-F*.

Discussion

We and others have recently shown that astrocytes derived from individuals with ALS are toxic to MNs^{13,14,44}. These findings add to the growing evidence that non-cell autonomous mechanisms contribute to MN death in ALS, and point to a crucial role of glia in ALS pathogenesis^{11,12}. However the mechanisms behind ALS astrocyte toxicity and selectivity towards MNs remain unknown. The understanding of these mechanisms is required to develop therapies aiming at delaying or even preventing MN degeneration in ALS. Our findings reported here show that ALS astrocytes recognize MNs as their targets based on the reduced expression of MHCI observed in MNs at later stages of disease in *SOD1*^{G93A} mouse model as well in ALS autopsy material. The relatively stable levels of MHCI found in GABAergic neurons upon culture with ALS astrocytes helps explain why certain neuronal subtypes other than MNs are spared from the astrocyte toxicity. Interestingly, in ALS microglia do not cause down-regulation of MHCI in MNs, but still induce MN death²⁸, suggesting that the mechanisms for MN recognition by reduced level of MHCI are astrocyte specific within the glial population. Overall, along with previous reports suggesting possible involvement of MHCI in many neurologic disorders^{23,25,45,47}, our findings support the important role of MHCI molecules in the motor neuron degeneration occurring in ALS.

Further studies are necessary to precisely identify signals originating from the astrocytes and the molecular mechanism behind MHCI reduction in MNs upon contact with ALS astrocytes. Here, we showed soluble factors secreted from ALS astrocytes can down-regulate MN MHCI expression, and identify ER stress as a likely mechanism governing this down-regulation. ER dysfunction is a critical contributor to MHCI loss on various cell types⁴⁸. Indeed, in the *SOD1* mouse models, ER stress is one of the first phenotypic alterations detected in vulnerable MNs^{49,50}, and remains a prominent feature of post-mortem ALS subject spinal cord MNs⁵¹. Since down-regulation of MHCI may initiate cellular events to trigger ALS astrocyte toxicity, it is imperative to identify how ALS astrocytes cause ER stress in MNs. Among the potential candidates, misfolded SOD1 should be considered due to their known involvements towards ER stress^{35,52}.

Our results are in alignment with the finding that ALS astrocytes might develop aberrant characteristics to convey toxicity to MNs⁵³. Despite this, the observation that FALS and SALS astrocytes express predominantly a single killer cell immunoglobulin-like receptor, *KIR3DL2*, opens the possibility to find common molecules that have potential therapeutic strategy to ALS despite disease etiology. Due to its ability to interact with *KIR3DL2*⁴³, and the low frequency of polymorphisms among different human populations⁵⁴, *HLA-F* is a promising candidate. Strikingly, *HLA-F* protein expression was found to be down regulated in post-mortem samples of ALS spinal cord MNs, and sustained *HLA-F* expression in human MNs *in vitro* confers protection from both FALS and SALS astrocyte toxicity. These findings suggest viral vectors, such as AAVs that may be developed to treat CNS

disorders⁵⁵⁻⁵⁹ in order to deliver *HLA-F* to MNs and hamper astrocyte toxicity in the larger body of SALS individuals.

Online Methods

Animals

All procedures were performed in accordance with the NIH Guidelines on the care and use of vertebrate animals and approved by the Institutional Animal Care and Use Committee of the Research Institute at Nationwide Children's Hospital. Transgenic mice that expressed human *SOD1* carrying the G93A mutation (B6SJL-Tg*SOD1*^{G93A}), referred to here as *SOD1*^{G93A} mice, were obtained from Jackson Laboratories and maintained, characterized by the guidelines of Jackson Laboratory for the entire of animal study⁶⁰ (Bar Harbor, ME). Animals were bred at our facilities and were housed under light/dark (12:12 hour) cycle with food and water ad libitum. At each generation, animals were genotyped, *SOD1*^{G93A} transgene copy number were verified by quantitative PCR, prior to either the isolation of primary cells or the injection of AAV9. To minimize variability due to gender effects on survival and behavior analysis, only female mice were used for AAV9-*H2k* injection experiments. After genotyping, *SOD1*^{G93A} animals were randomly selected for AAV9 injections of control, *H2k* or *H2k*. In each litter, half of the animals were treated with AAV9-empty and half with AAV9-*H2k* or AAV9-*H2k*. All procedures were performed in accordance with the NIH Guidelines and were approved by the Nationwide Children's Research Institutional Animal Care and Use Committee. The numbers of mice used in each experiment varied are indicated in the figure legends.

SOD1^{G93A} mouse survival and behavioral analysis

Disease stages (previously described^{28,57}) included the following: "Pre-symptomatic stage," during which mice displayed no disease symptoms and were not yet at peak body weight; "Symptomatic-stage," during which mice showed overt symptoms characterized by tremors and hindlimb paralysis and showed a 10% or more decrease from the peak of body weight; "End-stage," during which animals exhibited forelimb and hindlimb paralysis and were unable to right themselves within 30 seconds after being placed on its back. "Disease onset" was defined as the age at which mice reach their peak body weight. "Disease progression" was defined as the time period between disease onset and end stage. Motor coordination was recorded using a rotarod instrument (Columbus Instruments, Columbus, OH), Three trials were performed on accelerating rotarod beginning at 5 rpm per minute twice a week. The time each mouse remained on the rod was recorded. Data collection and analysis was performed by a researcher that was blinded to the treatment of animal groups.

Isolation and culture of mouse glial cells

Astrocytes and microglia were isolated from 110-130 day old *SOD1*^{G93A} and wild-type B6SJL mice. Astrocyte cultures were prepared as previously described with minor modifications⁶¹. Briefly, spinal cords were enzymatically dissociated to single cells with a mixture of Papain (2.5 U/ml; Worthington Biochemical, Lakewood, NJ), Dispase grade II (1 U/ml; Boehringer Mannheim Corporation, Indianapolis, IN) and Dnase I (250 U/ml; Worthington Biochemical) for about 20 minutes. After filtration with a 70 µm nylon mesh,

cells were pelleted, and resuspended in DMEM/F12 (Invitrogen, Carlsbad, CA) which was supplemented with 10% fetal bovine serum (FBS, Invitrogen) and 0.2% N2 supplement (Invitrogen). The cells were then plated onto laminin coated 75 cm² tissue culture flasks. Upon confluence, flasks were shaken overnight in order to remove potential microglial cells and then were treated with cytosine arabinose (20 μM, Sigma-Aldrich, St. Louis, MO). Prior to use, astrocyte preparations were screened for the presence of CTLs and natural killer (NK) cells and were found to be devoid of them.

Microglia were isolated following a protocol previously described²⁸. Briefly, tissues were fragmented with a scalpel and incubated in enzymatic solution containing papain (2.5 U/ml; Worthington Biochemical) for 60 minutes at 37 °C. 20% FBS in Hank's Balanced Salt Solution (HBSS, Invitrogen) was applied to the tissue, and they were then centrifuged at 200×g for 4 minutes. Cell pellets were resuspended in 2 ml of DNase I (0.5 mg/ml, Worthington Biochemical) in HBSS and were incubated for 5 minutes at room temperature. Tissue was gently disrupted with fire-polished Pasteur pipettes, filtered through a 70 micron cell strainer, and centrifuged at 200×g for 4 minutes. Pellet was then resuspended in 20ml of 20% isotonic Percoll (GE healthcare) in HBSS. 20ml of pure HBSS was carefully laid on top the percoll layer and centrifugation was performed at 200×g for 20 minutes with slow acceleration and no brake. The pellet containing the mixed glial cell population was washed once with HBSS and was suspended in Dulbecco's modified Eagle's/F12 medium with GlutaMAX™ (DMEM/F12, Invitrogen) supplemented with 10% heat inactivated FBS, antibiotic-antimycotic (all from Life Technologies) and 5 ng/ml of carrier-free murine recombinant granulocyte and macrophage colony stimulating factor (GM-CSF) (R&D systems, Minneapolis, MN). Cell suspension was then plated on a poly-L-lysine (Sigma) coated plate and maintained at 37°C. The media was replaced every 3 days until the cells reached confluency. Microglia that formed a non-adherent, floating cell layer were collected, replated, and cultured for an extended period of time. Microglia were incubated for 3 days without GM-CSF before being re-plated for co-culture with MNs. Prior to analysis, microglia preparations were tested for the presence of CTLs and NK cells and were found to be devoid of them.

Mouse NPC isolation and differentiation into astrocytes

NPCs were isolated according to methods previously described^{29,62}. Briefly, spinal cords were enzymatically dissociated in the same way as described for astrocytes. The cell suspension obtained was then mixed with an equal volume of isotonic Percoll (GE Healthcare) and was centrifuged at 20,000×g for 30 minutes at room temperature. Cells from the low-buoyancy fraction (5-10 ml above the red blood cell layer) were harvested, washed thoroughly with D-PBS/PSF (Invitrogen) and plated in 60 mm uncoated plates. Cells were grown in growth medium (DMEM/F12, Invitrogen) with 1% N2 supplement (Invitrogen), 20 ng/ml of fibroblast growth factor-2 (FGF-2, Peprotech, Rocky Hill, NJ) and 20 ng/ml of endothelial growth factor (EGF, Peprotech). Cells were first grown as neurospheres and then were placed on a polyornithine-laminin (P/L)-coated plates, in which they grow as monolayer cultures. NPC cultures were found to be devoid of astrocytes, microglia, CTLs and NK cells contaminants. Once cultures were established, NPCs from wild-type and *SOD1*^{G93A} mice were used to generate astrocytes by withdrawing growth factors and

supplementing the medium with 10% FBS (astrocyte media). The media was changed every 2 days thereafter. Astrocytes were allowed to mature for 7 days prior to being used in the experiments described above. Highly enriched astrocyte cultures were obtained with no detectable levels of microglia, CTLs and NK cells.

Human post-mortem NPC derived astrocytes

Post-mortem spinal cords were obtained from the National Disease Research Interchange (NDRI, Philadelphia, PA) and from Dr. Fred Gage (Salk Institute, CA). Informed consent was obtained from all subjects. Receipt of human tissues was granted through Nationwide Children's Hospital Institutional Review Board (IRB08-00402) and all human samples were used in accordance with their approved protocols. Extensive phenotypic characterization of the cell lines used here has been previously described^{13,44}. Cells were grown on laminin-coated plates in astrocyte media supplemented 0.2% N2 supplement (Invitrogen). Media change occurred every 3 days, and cells were passaged when cultures reached 80% confluency. Human astrocyte cultures were found to be devoid of microglia, CTLs and NK cells.

iPSC generation

NPCs, expressing the MN Hb9::GFP reporter, obtained from wild-type and *SOD1*^{G93A} mice were converted to iPSCs. As previously described, retrovirus encoding OCT3/4 and KLF4 were sufficient to generate iPSC clones^{63,64}. 20 viral particles per cell were needed to efficiently reprogram the cells. Cells were cultured in the presence of NPC media for four days followed by a change to mouse embryonic stem cell (mESC) media with DMEM (Millipore, Billerica, MA), supplemented with 18% ES FBS (Invitrogen), L-glutamine (2mM, Invitrogen), nonessential amino acids (1x, Millipore), antibiotic-antimycotic (Invitrogen), 2-mercaptoethanol (Sigma), and recombinant LIF (100U/ml, Millipore). iPSC clones were morphologically similar to mouse ESCs (HBG3 cells, Thomas Jessell, Columbia University) and were obtained within two weeks. A wide panel of markers was used to compare ESCs with the newly generated iPSC lines.

Mouse MN differentiation

Mouse ESCs or iPSCs expressing Hb9::GFP reporter were cultured on top of inactivated mouse fibroblasts (Millipore). MN differentiation was induced by plating $1-2 \times 10^6$ cells per 10 cm dish in the presence of 2 μ M retinoic acid (Sigma-Aldrich) and 2 μ M purmorphamine (Calbiochem, Billerica, MA). After 5 days of differentiation, embryonic bodies were dissociated and sorted based on levels of GFP using a FACSVantage/DiVa sorter (BD Biosciences, Rockville, MD).

NPC differentiation into GABAergic neurons

Mouse NPCs were induced to differentiate into GABAergic neurons by supplementing growth medium with 0.1% FBS (Invitrogen), retinoic acid (1 μ M, Sigma-Aldrich), and forskolin (5 μ M, Sigma-Aldrich). Media were changed every day. Cultures were allowed to differentiate for 7 days prior to being used for experiments.

Co-culture of mouse astrocytes with mouse MNs

Astrocytes were plated at the density of 35,000 cells per well in 96-well plates coated with laminin. After 48 hours, FACS sorted GFP⁺ MNs were plated on top of the astrocyte monolayer at a density of 10,000 cells per well. Co-cultures were performed in MN media composed of DMEM/F12 (Invitrogen) supplemented with 5% horse serum (Equitech Bio, Kerrville, TX), 2% N2 supplement (Invitrogen), 2% B27 supplement (Invitrogen), 10 ng/ml GDNF (Invitrogen), 10 ng/ml BDNF (Invitrogen), 10 ng/ml CNTF (Invitrogen). Half of the media was replaced every other day, with the addition of fresh growth factors.

Sustained expression of MHCI molecules in mouse MNs

To express histocompatibility 2 subclass MHCI in MNs, a previously described protocol was followed, with minor modifications⁶⁵. Briefly, wild-type astrocytes were plated on a laminin-coated transwell (Corning, Lowell, MA) using MN media. After 24 hours, sorted GFP⁺ MNs were plated on a separate laminin-coated 96 well plate in media, conditioned by wild-type astrocytes. Four hours later, the transwell containing wild-type astrocytes was transferred into the MN plate, after verification that all MNs were fully attached and were starting to show neuritic extensions. The following day, the transwell of wild-type astrocytes was removed and the MNs were infected with Lv- *H2k*, *H2k* or *H2I* (40 viral particles per MN). Twelve hours post-infection, co-culture with wild-type astrocytes via transwell was resumed. After 72 hours, the transwell was removed and the co-culture experiments with wild-type and *SOD1*^{G93A} astrocytes were initiated. Experiments were performed independently by two investigators.

Astrocyte conditioned media

Astrocyte conditioned medium was prepared by co-culturing mouse MNs and mouse astrocytes for 120 hours. After removal of cell debris by centrifugation (500 ×g for 10 min), medium was supplemented with GDNF, CNTF and BDNF. This medium was added to MNs cultures and cultures were evaluated after 24 hours.

Co-culture of human astrocytes with human MNs expressing *HLA-F*

MNs were obtained by differentiating human ES cell-derived MN progenitors (Lonza, Walkersville, MD) following the manufacturer's instructions. MN progenitors were plated at a density of 10,000 cells per well in a laminin coated 96-well plate. 48 hours after plating, the cells were infected with adenovirus encoding *NGN2*, *ISL1*, and *LHX3* in order to enhance efficiency and shorten the time required for MN differentiation⁶⁶. After 10 days of MN differentiation, MNs were infected with lentivirus to overexpress *HLA-F* (20 viral particles per MN). 3 days after, 10,000 human astrocytes were added to each well. Co-cultures were allowed to continue for another 14 days, with half of the media being replaced every other day. Due to the limited number of MNs available at a time of study, astrocytes were randomly chosen and co-culture initiated.

Viral vectors

To knockdown *H2k^b* levels in MNs or GABAergic neurons, sequences from the RNAi Consortium lentiviral shRNA library were screened and the sequence 5' -

TAAAGAGAACTGAGGGCTCTG -3' was used. The sequence 5' - GCGTAGATGTCCGATAAGAA-3' was used for the scrambled shRNA control. Sequences were cloned into a lentiviral vectors. *H2k^b* cDNA was purchased from Genecopia (Rockville, MD) and referred to as *H2k*. *H2d^b* cDNA (NM_010380.3) was purchased from ThermoFisher (Pittsburgh, PA) and referred to as *H2k*. *H2-I^d* cDNA (NM_001267808.1) was synthesized by Genscript (Piscataway, NJ) referred to as *H2I*. To knockdown *KIR3DL2* in human ALS astrocytes, sequences from the RNAi Consortium lentiviral shRNA library were also screened and the sequence 5' -TAAAGGAGAAAGAAGAGGAGG -3' was used. The sequence 5' -GGGAGAAAGAAGGAGGATAAA-3' was used for the scrambled shRNA control. The *HLA-F* cDNA (NM_001098479.1) was purchased from Genecopia (Rockville, MD). The production and purification of the lentivirus were performed as previously reported²⁹.

MN cell viability

At various time points during the co-culture of mouse astrocytes and mouse MNs, cell survival, neuritic length and soma size of MNs were recorded using a fully automated IN CELL 6000 cell imager (GE Healthcare) as previously reported⁴⁴. Images were processed with the Developer and Analyzer software package (GE Healthcare). Otherwise noted, images shown represent 120 hours post co-culture. All counts were performed in triplicate and repeated at least three times.

AAV9 injection in *SOD1^{G93A}* mice

H2k^b or *H2d^b* cDNA sequence used in our *in vitro* experiments was cloned into a AAV9 vector that has been reported to transduce high levels of MNs in brain and spinal cords^{56,57}. Self-complementary AAV9 encoding no transgene (AAV9-empty), or GFP (AAV9-GFP) or *H2d^b* (AAV9-*H2k*) or *H2k^b* (AAV9-*H2k*) was produced by transient transfection procedures using a double-stranded AAV2-ITR-based CB vector, with a plasmid encoding Rep2Cap9 sequence as previously described along with an adenoviral helper plasmid pHelper (Stratagene, Santa Clara, CA) in 293 cells. Injections of AAV9 were performed directly to the cerebral spinal fluid (CSF) at postnatal day 1 by direct injection into the lateral ventricles. Injection was performed with laser-pulled borosilicate glass needles (Sutter Instruments, Novato, CA, O.D.: 1.2 mm, I.D.: 0.69 mm 10 cm length) as previously described⁵⁹. Animals received a total dose of 2.33×10^{13} vg/kg in to 4 μ l volume. To validate and minimize variability associated with the injection procedure, at least two fold ($n = 24$) of the minimum number of animals that the guidelines for preclinical animal research in ALS/MND suggests⁶⁷ was used for our survival studies.

RNA isolation and RT-PCR

RNA was harvested using the RT² q-PCR-grade RNA isolation kit (Qiagen, Frederick, MD) and total RNA was reverse transcribed with RT² First Strand Kit (Qiagen) according to the manufacturer's instructions. After ensuring all cDNAs were devoid of genomic DNA contamination, mouse and human gene transcripts were amplified using gene-specific primers described in Supplementary Table 4. For detection of MHC1 inhibitor receptor transcripts from the *Ly49* gene and killer-cell immunoglobulin-like receptors (KIRs) families, astrocytes were prepared by co-culturing with mouse MNs and RT-PCR was performed using primer sets previously described⁶⁸. Real-time quantitative PCR reactions

were performed using RT² Real-Time SYBR Green/Rox Master Mix (Qiagen, Frederick, MD). Each sample was run in triplicate and relative concentration was calculated using the ddCt values normalized to endogenous actin transcript.

***In situ* hybridization**

Spinal cords were removed from 60 day old wild-type mice and frozen in M1 embedding matrix (Shandon, Pittsburgh). The negative control, labeled with H2k^bd^b KO, was an *H2k^b-/-d^b-/-* double knockout as previously described²². Twelve μm cryostat sections were obtained, affixed to slides, air-dried, and stored at -80°C. *In situ* hybridization was performed as previously described^{22,69}. Briefly, slides were thawed and fixed in 4% paraformaldehyde before proteinase K (1 μg/ml) treatment. Slides were then acetylated and dehydrated in an ethanol series (50%, 75%, 2 X 95%, and 2X 100%). Labeled (α-³⁵S-UTP) riboprobe was diluted to 0.75 × 10⁷ cpm/ml in 1X Denhardt's solution with 50% deionized formamide, 10% dextran sulfate, 0.3 M NaCl, 10 mM Tris-HCl pH 8.0, and 1 mM EDTA pH 8.0; applied to sections; and then hybridization took place at 62°C for 12–18 h. After hybridization, coverslips were floated off in 4× SSC, and then treated with 50 μg/ml RNase A for 30 min at 37°C. Slides were washed with a series of SSC solutions, beginning at 2X and concluding with a high-stringency wash of 0.1X SSC (0.15 M sodium chloride/0.015 M sodium citrate, pH 7) at 60°C for 30 min. Finally, sections were dehydrated through an ethanol series and placed on film. After exposure to Kodak XAR-5 film at room temperature, sections were coated with NTB-2 emulsion and developed after 2–4 weeks.

The sequence of the *H2d^b* probe was: 3' -
 AGGTGGGCTACGTGGACGACGAGGAGTTCGTGCGCTTCGACAGCGACGCGGAGA
 ATCCGAGATATGAGCCGCGGGCGCCGTGGATGGAGCAGGAGGGGCCGGAGTATT
 GGGAGCGGGAACACAGAAAGCCAAGGGCCAAGAGCAGTGGTTCCGAGTGAGC
 C
 TGAGGAACCTGCTCGGCTACTACAACCAGAGCGCGGGCGGCTCTCACACTCCA
 GCAGATGTCTGGCTGTGACTTGGGGTCCGACTGGCGCCTCCTCCGCGGGTACCT
 CGAGTTCGCCTATGAAGGCCGCGATTACATCGCCCTGAACGAGAACCCAC-5' .

Adjacent sections were hybridized with sense and antisense probes. No specific hybridization was seen using sense probes.

Fixation and immunostaining

Cells were fixed with 4% paraformaldehyde (PFA) for 10 min. Mouse spinal cords were obtained by intracardiac perfusion with 4% PFA followed by 24 hours of post-fixation. Spinal cords were rinsed twice with 0.1 M sodium phosphate buffer and immersed in 30% sucrose for 2 days at 4°C or until the spinal cords sank to the bottom of the 50ml conical. Fixed spinal cords were embedded and sectioned using a vibratome (40 μm). For antigen detection using frozen sections, mouse spinal cord tissues were cut in 5- to 6-mm sections and embedded in Tissue-Tek OCT compound (Sakura Finetek) and frozen with dry ice. Tissues were then sectioned at 10 μm with a cryostat, collected directly on gelatinized objective slides and then stored at -20 °C before immunocytochemical analysis. Paraffin-embedded human spinal cord tissues were obtained from NDRI and from Dr. Jonathan Glass

and Dr. Marla Gearing (Emory University, GA), which had obtained informed consent from all prospective donors. Tissues were sectioned at 10 μ m and antigen retrieval methods were applied based on manufacturer's suggestions where primary antibodies were purchased. Staining of control and experimental groups was always performed in parallel. Antibodies used are listed in Supplementary Table 1. For most antigens, samples were first incubated for 1 hour in TBS containing 0.1% triton-X and 10% donkey serum, followed by incubation with the primary antibody for 48-72 hours at 4°C. For Ly49C/I staining, frozen sections previously prepared on slides were washed with TBS three times, then incubated for two hours in TBS containing 5% donkey serum, followed by incubation with primary antibody for 72 hours at 4°C. detection with cyanine dyes (Cy2, Cy3, and Cy5) labeled secondary antibodies used at the dilution of 1:250 (Jackson immunoresearch, West Grove, PA) was performed for 2 hours at room temperature.

MHCI staining was performed according to a previously described protocol, with minor modifications^{25,46}. The antibody ER-HR52 recognizes histocompatibility 2 subclasses for mouse classical MHC I molecules (H2k^bd^b) and the antibody EMR8-5 recognizes all HLA-A, B and C of the human classical MHC I molecules (HLA-ABC), therefore we refer to it in the text as MHC I. *HLA-F* expression was probed with a rabbit-anti-*HLA-F* antibody^{75,76}. Membrane and cytoplasmic expression of *HLA-F* was interpreted as positive. Briefly, for *in vitro* MHC I labeling, cells on coverslips were fixed, blocked and incubated with primary and secondary antibodies without membrane permeabilization during the staining process. MHC I levels were obtained from randomly selected MNs using confocal microscope. MHC I fluorescence intensity values per MN were automatically measured using Adobe Photoshop CS5 extended version (Adobe, San Jose, CA) and were corrected to soma size and GFP expression of cells analyzed. For *in vivo* MHC I labelling, cell permeabilization was achieved using 0.05% triton-X for mouse spinal cord samples and 0.1% saponin for human spinal cord samples for 30 minutes at room temperature. Incubation with primary and secondary antibodies was performed in 10% donkey serum without any detergent. Detection of MHC I in paraffin embedded human tissue was achieved with 3,3' -diaminobensidine staining by using the ABC and VectorRed Kit protocols (Vector Laboratories, Burlingame, CA). Tissues were counterstained with Hematoxylin QS solution (Vector Laboratories). Fluorescence images were captured on a laser scanning confocal microscope (Carl Zeiss Microscopy, Thornwood, NY) and 3,3' -diaminobensidine stained images were captured with the Zeiss Axioscope. Evaluation of MHC I levels in MNs were performed by an operator blinded to the identity of sample been evaluated.

Statistical analysis

Statistical analysis was performed using Graph Pad Prism 6 software (La Jolla). Depending on the number of variables and time-points in each experiment, statistical analysis of mean differences between groups was performed by either Student's t-test or multiway ANOVA followed by a Bonferroni post hoc analysis. Kaplan-Meier survival analyses were analyzed by the log-rank test. Comparison of mean survival, disease onset and progression were analyzed by the unpaired *t* test. Specific statistical tests, *P* values and sample size are indicated in figure legends.

Supplementary Material

Refer to Web version on PubMed Central for supplementary material.

Acknowledgements

We would like to thank C. Shatz (Stanford University) for critical discussions, S. Eckardt for expert editorial assistance, The National Disease Research Institute (NDRI), A. Burghes (The Ohio State University), J. R. Mendell (Nationwide Children's), J. Glass and M. Gearing (Emory University supported by NIH/NINDS P30NS055077) for providing human spinal cord specimens, F. Gage (Salk Institute) for providing human post-mortem NPCs used to generate non-ALS astrocytes, M. Hester for guidance with iPSC generation, and K. Campbell for technical assistance. This work was supported by the US National Institutes of Health (NIH) grant R01-NS644912, RC2-NS69476, and funding from the Robert Packard Center for ALS Research, the Project A.L.S. and the Helping Link Foundation. Authors part of this work also received research fellowships from the Swiss National Science Foundation, the Marie Curie Foundation, NINDS Training in Neuromuscular Disease, The Ohio State University Presidential Fellowship and The Ohio State University and Nationwide Children's Hospital Muscle Group Fellowship.

References

1. Hardiman O, van den Berg LH, Kiernan MC. Clinical diagnosis and management of amyotrophic lateral sclerosis. *Nat Rev Neurol*. 2011; 7:639–649. [PubMed: 21989247]
2. Brown RH Jr. Amyotrophic lateral sclerosis. Insights from genetics. *Arch Neurol*. 1997; 54:1246–1250. [PubMed: 9341570]
3. Kwiatkowski TJ Jr, et al. Mutations in the FUS/TLS gene on chromosome 16 cause familial amyotrophic lateral sclerosis. *Science*. 2009; 323:1205–1208. [PubMed: 19251627]
4. Rosen DR, et al. Mutations in Cu/Zn superoxide dismutase gene are associated with familial amyotrophic lateral sclerosis. *Nature*. 1993; 362:59–62. [PubMed: 8446170]
5. Sreedharan J, et al. TDP-43 mutations in familial and sporadic amyotrophic lateral sclerosis. *Science*. 2008; 319:1668–1672. [PubMed: 18309045]
6. Van Deerlin VM, et al. TARDBP mutations in amyotrophic lateral sclerosis with TDP-43 neuropathology: a genetic and histopathological analysis. *Lancet Neurol*. 2008; 7:409–416. [PubMed: 18396105]
7. Vance C, et al. Mutations in FUS, an RNA processing protein, cause familial amyotrophic lateral sclerosis type 6. *Science*. 2009; 323:1208–1211. [PubMed: 19251628]
8. Bosco DA, et al. Wild-type and mutant SOD1 share an aberrant conformation and a common pathogenic pathway in ALS. *Nature neuroscience*. 2010; 13:1396–1403. [PubMed: 20953194]
9. Gruzman A, et al. Common molecular signature in SOD1 for both sporadic and familial amyotrophic lateral sclerosis. *Proceedings of the National Academy of Sciences of the United States of America*. 2007; 104:12524–12529. [PubMed: 17636119]
10. Gurney ME, et al. Motor neuron degeneration in mice that express a human Cu,Zn superoxide dismutase mutation. *Science*. 1994; 264:1772–1775. [PubMed: 8209258]
11. Ilieva H, Polymenidou M, Cleveland DW. Non-cell autonomous toxicity in neurodegenerative disorders: ALS and beyond. *J Cell Biol*. 2009; 187:761–772. [PubMed: 19951898]
12. Philips T, Rothstein JD. Glial cells in amyotrophic lateral sclerosis. *Exp Neurol*. 2014
13. Haidet-Phillips AM, et al. Astrocytes from familial and sporadic ALS patients are toxic to motor neurons. *Nat Biotechnol*. 2011; 29:824–828. [PubMed: 21832997]
14. Re DB, et al. Necroptosis drives motor neuron death in models of both sporadic and familial ALS. *Neuron*. 2014; 81:1001–1008. [PubMed: 24508385]
15. Boulanger LM. Immune proteins in brain development and synaptic plasticity. *Neuron*. 2009; 64:93–109. [PubMed: 19840552]
16. Tian L, Ma L, Kaarela T, Li Z. Neuroimmune crosstalk in the central nervous system and its significance for neurological diseases. *Journal of neuroinflammation*. 2012; 9:155. [PubMed: 22747919]

17. Needleman LA, Liu XB, El-Sabeawy F, Jones EG, McAllister AK. MHC class I molecules are present both pre- and postsynaptically in the visual cortex during postnatal development and in adulthood. *Proceedings of the National Academy of Sciences of the United States of America*. 2010; 107:16999–17004. [PubMed: 20837535]
18. Fourgeaud L, et al. MHC class I modulates NMDA receptor function and AMPA receptor trafficking. *Proceedings of the National Academy of Sciences of the United States of America*. 2010; 107:22278–22283. [PubMed: 21135233]
19. Goddard CA, Butts DA, Shatz CJ. Regulation of CNS synapses by neuronal MHC class I. *Proceedings of the National Academy of Sciences of the United States of America*. 2007; 104:6828–6833. [PubMed: 17420446]
20. Huh GS, et al. Functional requirement for class I MHC in CNS development and plasticity. *Science*. 2000; 290:2155–2159. [PubMed: 11118151]
21. Lee H, et al. Synapse elimination and learning rules co-regulated by MHC class I H2-Db. *Nature*. 2014; 509:195–200. [PubMed: 24695230]
22. McConnell MJ, Huang YH, Datwani A, Shatz CJ. H2-K(b) and H2-D(b) regulate cerebellar long-term depression and limit motor learning. *Proceedings of the National Academy of Sciences of the United States of America*. 2009; 106:6784–6789. [PubMed: 19346486]
23. Freria CM, Zanon RG, Santos LM, Oliveira AL. Major histocompatibility complex class I expression and glial reaction influence spinal motoneuron synaptic plasticity during the course of experimental autoimmune encephalomyelitis. *J Comp Neurol*. 2010; 518:990–1007. [PubMed: 20127802]
24. Kim T, et al. Human LILRB2 is a beta-amyloid receptor and its murine homolog PirB regulates synaptic plasticity in an Alzheimer's model. *Science*. 2013; 341:1399–1404. [PubMed: 24052308]
25. Nardo G, et al. Transcriptomic indices of fast and slow disease progression in two mouse models of amyotrophic lateral sclerosis. *Brain*. 2013; 136:3305–3332. [PubMed: 24065725]
26. Staats KA, et al. Beta-2 microglobulin is important for disease progression in a murine model for amyotrophic lateral sclerosis. *Front Cell Neurosci*. 2013; 7:249. [PubMed: 24368896]
27. Linda H, Hammarberg H, Piehl F, Khademi M, Olsson T. Expression of MHC class I heavy chain and beta2-microglobulin in rat brainstem motoneurons and nigral dopaminergic neurons. *J Neuroimmunol*. 1999; 101:76–86. [PubMed: 10580816]
28. Frakes AE, et al. Microglia induce motor neuron death via the classical NF-kappaB pathway in amyotrophic lateral sclerosis. *Neuron*. 2014; 81:1009–1023. [PubMed: 24607225]
29. Miranda CJ, et al. Aging brain microenvironment decreases hippocampal neurogenesis through Wnt-mediated survivin signaling. *Aging Cell*. 2012
30. Clarke LE, Barres BA. Emerging roles of astrocytes in neural circuit development. *Nature reviews. Neuroscience*. 2013; 14:311–321. [PubMed: 23595014]
31. Liu J, et al. The expression pattern of classical MHC class I molecules in the development of mouse central nervous system. *Neurochemical research*. 2013; 38:290–299. [PubMed: 23161087]
32. Israelson A, et al. Macrophage Migration Inhibitory Factor as a Chaperone Inhibiting Accumulation of Misfolded SOD1. *Neuron*. 2015; 86:218–232. [PubMed: 25801706]
33. Marchetto MC, et al. Non-cell-autonomous effect of human SOD1 G37R astrocytes on motor neurons derived from human embryonic stem cells. *Cell Stem Cell*. 2008; 3:649–657. [PubMed: 19041781]
34. Nagai M, et al. Astrocytes expressing ALS-linked mutated SOD1 release factors selectively toxic to motor neurons. *Nature neuroscience*. 2007; 10:615–622. [PubMed: 17435755]
35. Nishitoh H, et al. ALS-linked mutant SOD1 induces ER stress- and ASK1-dependent motor neuron death by targeting Derlin-1. *Genes & development*. 2008; 22:1451–1464. [PubMed: 18519638]
36. Dodge JC, et al. Delivery of AAV-IGF-1 to the CNS extends survival in ALS mice through modification of aberrant glial cell activity. *Molecular therapy : the journal of the American Society of Gene Therapy*. 2008; 16:1056–1064. [PubMed: 18388910]
37. Chakrabarty P, et al. Capsid serotype and timing of injection determines AAV transduction in the neonatal mice brain. *PLoS One*. 2013; 8:e67680. [PubMed: 23825679]

38. Robbins KL, Glascock JJ, Osman EY, Miller MR, Lorson CL. Defining the therapeutic window in a severe animal model of spinal muscular atrophy. *Hum Mol Genet.* 2014; 23:4559–4568. [PubMed: 24722206]
39. Tay CH, Szomolanyi-Tsuda E, Welsh RM. Control of infections by NK cells. *Current topics in microbiology and immunology.* 1998; 230:193–220. [PubMed: 9586357]
40. Lanier LL. NK cell recognition. *Annual review of immunology.* 2005; 23:225–274.
41. Long EO. Regulation of immune responses through inhibitory receptors. *Annual review of immunology.* 1999; 17:875–904.
42. Chiu IM, et al. T lymphocytes potentiate endogenous neuroprotective inflammation in a mouse model of ALS. *Proceedings of the National Academy of Sciences of the United States of America.* 2008; 105:17913–17918. [PubMed: 18997009]
43. Goodridge JP, Burian A, Lee N, Geraghty DE. HLA-F and MHC class I open conformers are ligands for NK cell Ig-like receptors. *J Immunol.* 2013; 191:3553–3562. [PubMed: 24018270]
44. Meyer K, et al. Direct conversion of patient fibroblasts demonstrates non-cell autonomous toxicity of astrocytes to motor neurons in familial and sporadic ALS. *Proc Natl Acad Sci U S A.* 2014; 111:829–832. [PubMed: 24379375]
45. Oliveira AL, et al. A role for MHC class I molecules in synaptic plasticity and regeneration of neurons after axotomy. *Proceedings of the National Academy of Sciences of the United States of America.* 2004; 101:17843–17848. [PubMed: 15591351]
46. Thams S, et al. Classical major histocompatibility complex class I molecules in motoneurons: new actors at the neuromuscular junction. *J Neurosci.* 2009; 29:13503–13515. [PubMed: 19864563]
47. Rivera-Quinones C, et al. Absence of neurological deficits following extensive demyelination in a class I-deficient murine model of multiple sclerosis. *Nat Med.* 1998; 4:187–193. [PubMed: 9461192]
48. Hansen TH, Bouvier M. MHC class I antigen presentation: learning from viral evasion strategies. *Nat Rev Immunol.* 2009; 9:503–513. [PubMed: 19498380]
49. Saxena S, Cabuy E, Caroni P. A role for motoneuron subtype-selective ER stress in disease manifestations of FALS mice. *Nature neuroscience.* 2009; 12:627–636. [PubMed: 19330001]
50. Filezac de L'Etang A, et al. Marinesco-Sjogren syndrome protein SIL1 regulates motor neuron subtype-selective ER stress in ALS. *Nature neuroscience.* 2015; 18:227–238. [PubMed: 25559081]
51. Lautenschlaeger J, Prell T, Grosskreutz J. Endoplasmic reticulum stress and the ER mitochondrial calcium cycle in amyotrophic lateral sclerosis. *Amyotroph Lateral Scler.* 2012; 13:166–177. [PubMed: 22292840]
52. Kikuchi H, et al. Spinal cord endoplasmic reticulum stress associated with a microsomal accumulation of mutant superoxide dismutase-1 in an ALS model. *Proceedings of the National Academy of Sciences of the United States of America.* 2006; 103:6025–6030. [PubMed: 16595634]
53. Diaz-Amarilla P, et al. Phenotypically aberrant astrocytes that promote motoneuron damage in a model of inherited amyotrophic lateral sclerosis. *Proceedings of the National Academy of Sciences of the United States of America.* 2011; 108:18126–18131. [PubMed: 22010221]
54. Moscoso J, Serrano-Vela JI, Pacheco R, Arnaiz-Villena A. HLA-G, -E and -F: allelism, function and evolution. *Transpl Immunol.* 2006; 17:61–64. [PubMed: 17157219]
55. Bevan AK, et al. Systemic gene delivery in large species for targeting spinal cord, brain, and peripheral tissues for pediatric disorders. *Molecular therapy : the journal of the American Society of Gene Therapy.* 2011; 19:1971–1980. [PubMed: 21811247]
56. Foust KD, et al. Intravascular AAV9 preferentially targets neonatal neurons and adult astrocytes. *Nat Biotechnol.* 2009; 27:59–65. [PubMed: 19098898]
57. Foust KD, et al. Therapeutic AAV9-mediated suppression of mutant SOD1 slows disease progression and extends survival in models of inherited ALS. *Mol Ther.* 2013; 21:2148–2159. [PubMed: 24008656]
58. Miyazaki Y, et al. Viral delivery of miR-196a ameliorates the SBMA phenotype via the silencing of CELF2. *Nat Med.* 2012; 18:1136–1141. [PubMed: 22660636]

59. Meyer K, et al. Improving single injection CSF delivery of AAV9-mediated gene therapy for SMA: a dose-response study in mice and nonhuman primates. *Molecular therapy : the journal of the American Society of Gene Therapy*. 2015; 23:477–487. [PubMed: 25358252]
60. Melanie Leitner SM. Cathleen Lutz. Working with ALS Mice (Guidelines for preclinical testing & colony management). Manual in Jackson Laboratory. 2009
61. Noble, M.; Mayer-Proschel, M. Culture of astrocytes, oligodendrocytes, and O-2A progenitor cells. MIT press; Cambridge: 1998.
62. Ray J, Gage FH. Differential properties of adult rat and mouse brain-derived neural stem/progenitor cells. *Mol Cell Neurosci*. 2006; 31:560–573. [PubMed: 16426857]
63. Hester ME, et al. Two factor reprogramming of human neural stem cells into pluripotency. *PLoS One*. 2009; 4:e7044. [PubMed: 19763260]
64. Kim JB, et al. Pluripotent stem cells induced from adult neural stem cells by reprogramming with two factors. *Nature*. 2008; 454:646–650. [PubMed: 18594515]
65. Kaech S, Banker G. Culturing hippocampal neurons. *Nat Protoc*. 2006; 1:2406–2415. [PubMed: 17406484]
66. Hester ME, et al. Rapid and efficient generation of functional motor neurons from human pluripotent stem cells using gene delivered transcription factor codes. *Mol Ther*. 2011; 19:1905–1912. [PubMed: 21772256]
67. Ludolph AC, et al. Guidelines for preclinical animal research in ALS/MND: A consensus meeting. *Amyotrophic lateral sclerosis : official publication of the World Federation of Neurology Research Group on Motor Neuron Diseases*. 2010; 11:38–45.
68. Thompson A, van der Slik AR, Koning F, van Bergen J. An improved RTPCR method for the detection of killer-cell immunoglobulin-like receptor (KIR) transcripts. *Immunogenetics*. 2006; 58:865–872. [PubMed: 17033821]
69. Syken J, Shatz CJ. Expression of T cell receptor beta locus in central nervous system neurons. *Proc Natl Acad Sci U S A*. 2003; 100:13048–13053. [PubMed: 14569018]

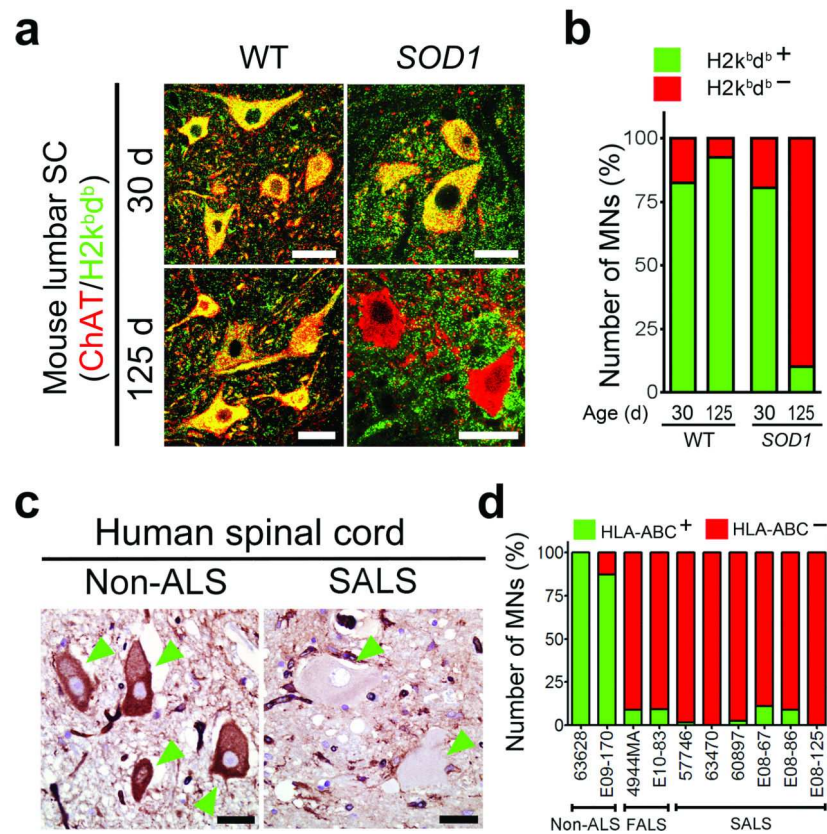


Figure 1. MHC I expression is reduced on spinal MNs in end-stage ALS

(a) Representative immunofluorescence images (from three images evaluated) showing MHC I ($H2d^b/H2k^b$) expression in MNs at 30 and 125 days in $SOD1^{G93A}$ mice. (b) Percent of MHC I positive lumbar spinal cord MNs in $SOD1^{G93A}$ and control mice evaluated as shown in (a) For each group, two animals were used and MNs counts were pulled together. 321, 216, 216, 154 MNs were counted in graph columns 1 through 4. (c) Immunohistochemical analysis of MHC I (HLA-ABC) expression in spinal MNs of individuals with ALS post-mortem. Green arrowheads point to MNs. (d) Percent of MHC I positive MNs in the spinal cords of individuals with ALS individuals and controls determined as shown in (c). For analysis two non-ALS, two FALS and 6 SALS individuals were analyzed. 50, 60, 35, 51, 71, 87, 45, 46, 68 and 22 of MNs were counted in graph columns 1 through 10. WT, wild-type mouse. $SOD1$, $SOD1^{G93A}$ mouse. Scale bars 20 μ m.

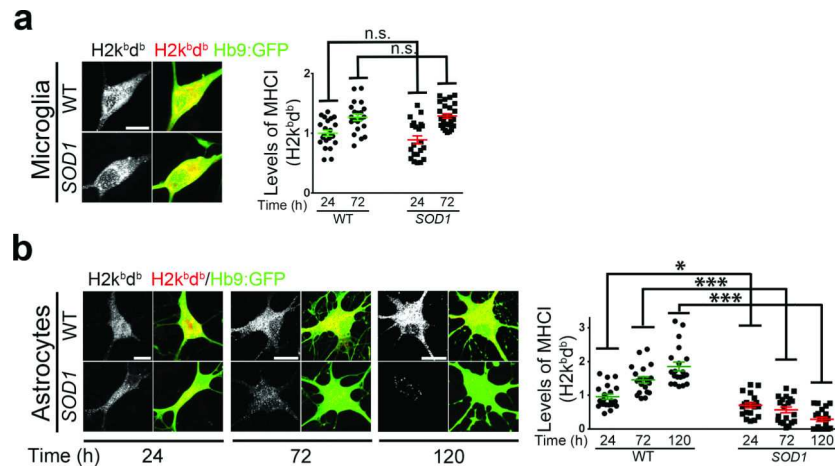


Figure 2. ALS astrocytes induce down-regulation of MHCI expression in MNs

(a,b) Representative immunofluorescence images (of three independent experiments) showing MHCI (*H2d^b/H2k^b*) expression in MNs cultured in the presence of either wild type or *SOD1^{G93A}* microglia for 72 hours (a) and measurement of their MHCI expression relative to levels found in MNs cultured with wild type microglia for 24h (b). (c,d) Representative immunofluorescence images (of three independent experiments) showing MHCI (*H2d^b/H2k^b*) expression in MNs cultured in the presence of either wild type or *SOD1^{G93A}* astrocytes during a 120 hours period (c) and measurement of their MHCI expression relative to levels found in MNs cultured with wild type astrocytes for 24h (d). Experiments were made in triplicate. Levels of MHCI are expressed as mean fluorescence intensity (MFI) found in MNs. Error bars represent s.e.m.. Each dot in graphs (b and d) represents MHCI level found per MN (One-Way ANOVA, *P<0.05; ***P<0.001; n.s., non-significant P 0.05). WT, wild-type mouse. *SOD1*, *SOD1^{G93A}* mouse. Scale bars 10 μ m.

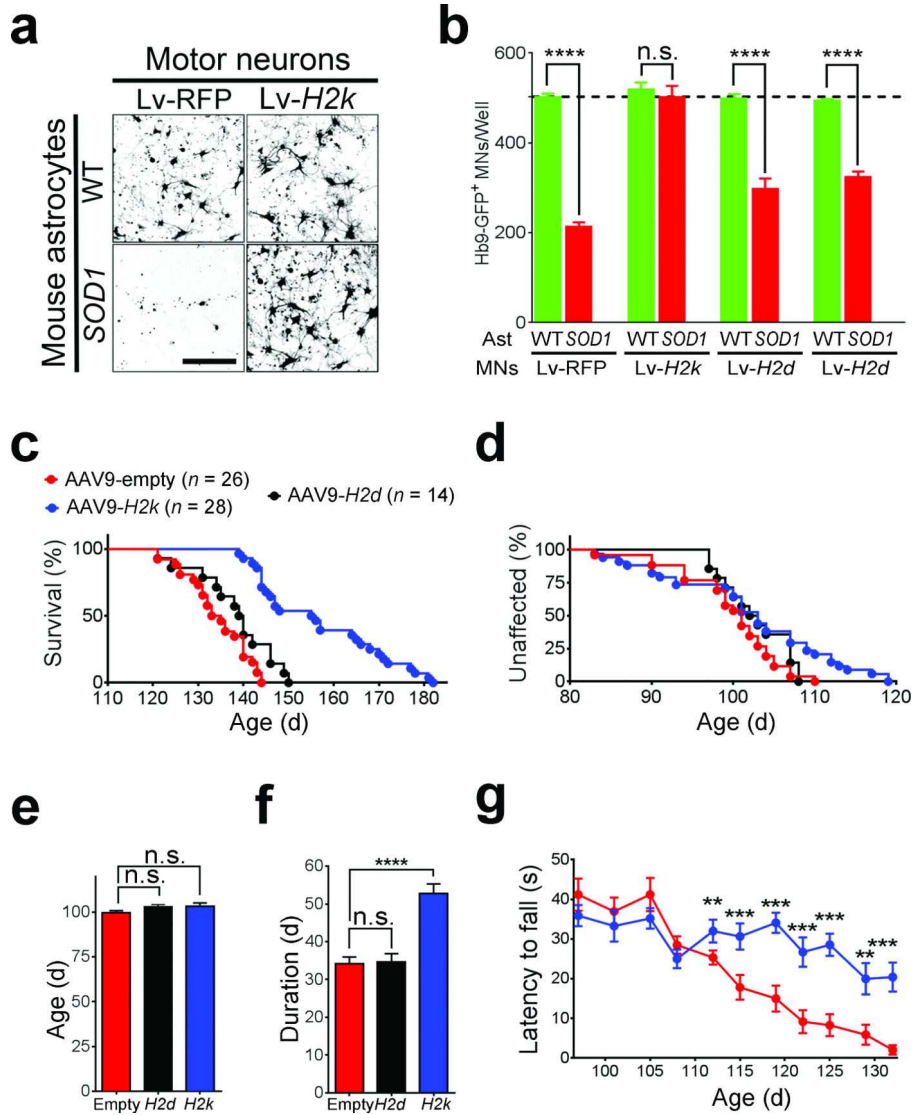


Figure 3. *H2k^b* expression protects MNs from ALS astrocyte-induced toxicity and delays disease progression in *SOD1^{G93A}* mice

(a) Representative immunofluorescence images (of three independent experiments) of MNs expressing either RFP or *H2k* and cultured in the presence of wild type or *SOD1^{G93A}* astrocytes for 120 hours. Scale bar 100 μ m. (b) Survival of MNs expressing either, RFP, *H2k*, *H2k* or *H2l* and cultured in the presence of wild type or *SOD1^{G93A}* astrocytes for 120 hours. Data shown is a representative of three independent experiments and is displayed as the mean \pm s.e.m of counts three replicates (**** $P < 0.0001$; n.s., non-significant, one-Way ANOVA). (c) Kaplan-Meier survival curve of female *SOD1^{G93A}* mice treated with AAV9-*H2k* ($n = 28$), AAV9-*H2k* ($n = 14$) or AAV9-empty controls ($n = 26$). Mean survival, AAV9-*H2k* 156.9 ± 2.6 , AAV9-*H2k* 139.2 ± 1.4 , AAV9-empty 135.5 ± 1.6 days, mean \pm s.e.m, $P < 0.0001$, unpaired *t*-test. (d,e) Age of onset observed in AAV9 treated *SOD1^{G93A}* mice and displayed by the Kaplan-Meier curve (d) and the mean age of onset (e). AAV9-*H2k* 103.3 ± 2.0 , AAV9-*H2k* 103.1 ± 1.2 days, AAV9-empty 99.73 ± 1.2 , mean \pm s.e.m, $P = 0.1$, unpaired *t*-test. (f) Mean disease progression observed in AAV9 treated *SOD1^{G93A}* mice.

AAV9-*H2k*, 52.7 ± 2.6 ; AAV9-*H2k*, 34.62 ± 2.2 ; AAV9-empty 34.1 ± 1.8 days, mean \pm s.e.m, $P < 0.0001$, unpaired *t*-test. (g) Rotarod performance of AAV9-*H2k* treated *SOD1*^{G93A} mice compared with age-matched controls, mean \pm s.e.m, * $P < 0.05$; ** $P < 0.01$; *** $P < 0.005$, unpaired *t*-test. WT, wild-type. *SOD1*, *SOD1*^{G93A}. Ast, astrocytes.

Author Manuscript

Author Manuscript

Author Manuscript

Author Manuscript

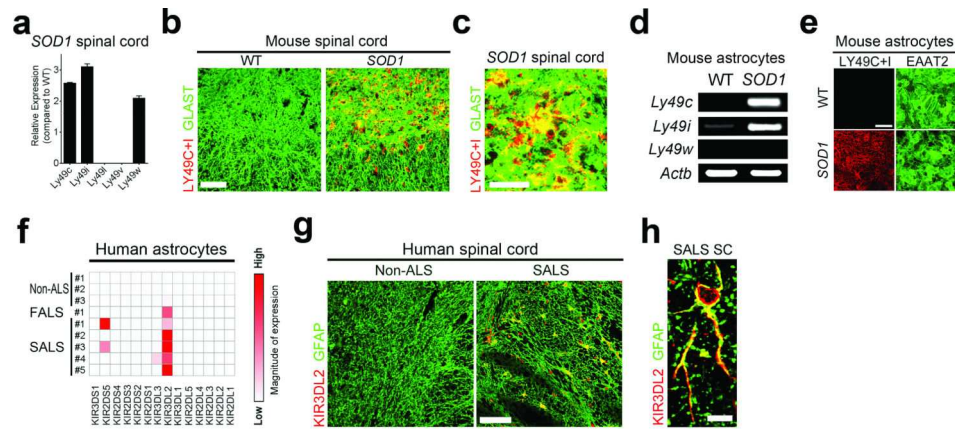


Figure 4. ALS astrocytes express MHCII inhibitory receptors

(a-e) Evaluation of the expression of MHCII inhibitory receptors found in *SOD1*^{G93A} mice spinal cord at disease end-stage (a-c) or astrocytes lines (d-e), by RNA analysis (a,d) or immunohistochemistry analysis (b,c,e). (f-h) Expression of the MHCII inhibitory receptor *KIR3DL2* in human ALS astrocytes cell lines as determined by RNA analysis (f) and in sections of spinal cord from SALS post-mortem tissue (g-h). Data presented in (a-h) is a representative of finding from three independent experiments. WT, wild-type. *SOD1*, *SOD1*^{G93A}. Scale bars 50 μ m (b), 200 μ m (e, g), 10 μ m (c), 5 μ m (h).

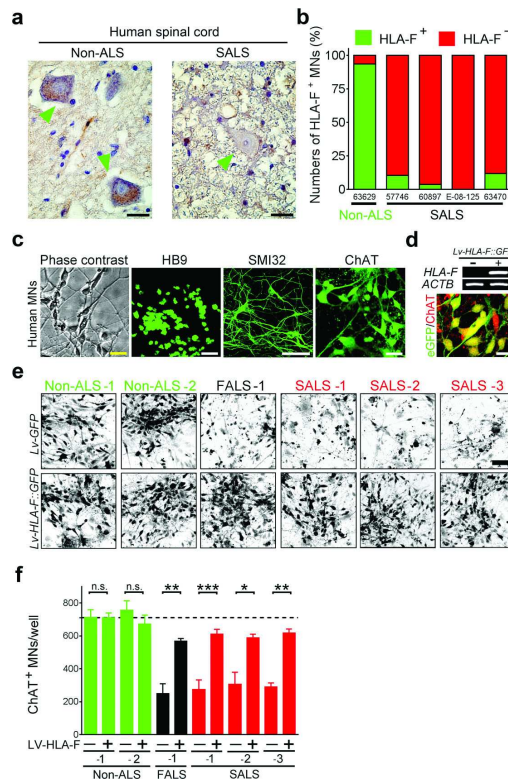


Figure 5. *HLA-F* expression protects human MNs from ALS astrocyte-induced toxicity
(a) Representative images (from three independent experiments) of immunohistochemistry analysis performed in human spinal cord tissue probing for *HLA-F* expression. Green arrowheads point to MNs. *HLA-F* was visualized by 3,3'-Diaminobenzidine (DAB) staining.
(b) Percent of *HLA-F* positive MNs found in human spinal cords of ALS individuals and control determined as shown in **(a)**. For columns 1 through 5, the total number of MNs was 62, 58, 54, 26 and 42, respectively. Scale bars 20 μ m. Number at the bottom of the columns represent subject ID number.
(c) Microscope images of human ESC derived MNs used to evaluate morphology and expression of prototypic MN markers.
(d) RNA (**upper panel**) and immunocytochemistry analysis (**lower panel**) of lentivirus infected cells displaying *HLA-F* and eGFP expression in human MNs.
(e) Representative images (from three independent experiments) of human MNs expressing *HLA-F* and co-cultured with FALS and SALS astrocyte visualized by ChAT staining.
(f) Quantification of the number of surviving MNs as shown in **(e)**. Dotted line represents average MN counts when co-cultured with non-ALS controls. Data shows a representative of three independent experiments and is displayed as the mean \pm s.e.m counts of triplicates. (One-Way ANOVA, * $P < 0.05$; ** $P < 0.01$; *** $P < 0.001$; ns, non-significant $P > 0.5$). Scale bars 20 μ m (**a**), 50 μ m (**c-d**), 100 μ m (**e**).